

INVESTIGATION OF THE EFFECT OF SHOCK ON  
THE ANTARCTIC METEORITES BY THE  
 $^{40}\text{Ar}$ - $^{39}\text{Ar}$  METHOD

Yutaka TAKIGAMI and Ichiro KANEOKA\*

*Geophysical Institute, Faculty of Science, University of Tokyo,  
11-16, Yayoi 2-chome, Bunkyo-ku, Tokyo 113*

**Abstract:** In order to investigate the shock effect on the  $^{40}\text{Ar}$ - $^{39}\text{Ar}$  ages of meteorites,  $^{40}\text{Ar}$ - $^{39}\text{Ar}$  geochronological studies were performed on two Antarctic meteorites, Y-790964 (LL, shocked) and Y-790448 (LL3, unshocked). Samples were taken from the inner and the outer parts of each meteorite for comparison.

The inner part and two outer parts of the seriously shocked Y-790964 have almost the same plateau ages of  $1276 \pm 24$  Ma,  $1264 \pm 23$  Ma and  $1241 \pm 37$  Ma. Older ages are not observed in the higher temperature fractions, which would indicate a very intense shock event. In the unshocked meteorite, Yamato-790448, the plateau-like ages of about 4492 Ma for the inner part and 4325 Ma for the outer part are observed at lower temperatures, but the reason for the apparent difference of the ages is not yet clear.

## 1. Introduction

In order to determine the age of a shock event on a meteorite by the K-Ar and  $^{40}\text{Ar}$ - $^{39}\text{Ar}$  methods, a portion of the meteorite is commonly used (*e.g.* PODOSEK, 1972; BOGARD *et al.*, 1976). In such a case, it is implied that the portion would represent the whole meteorite concerned. When the meteorite is affected seriously by the impact event, however, it is not clear whether the meteorite would still keep its homogeneity or not from the petrological point of view. Accordingly, a question arises whether the K-Ar or  $^{40}\text{Ar}$ - $^{39}\text{Ar}$  age for a part of the meteorite surely represents the age of the shock event for the whole meteorite. Hence, in order to check this problem, the  $^{40}\text{Ar}$ - $^{39}\text{Ar}$  ages against the degassing temperatures were compared among the different parts of the same shocked meteorite and the unshocked one.

## 2. Samples

A shocked and an unshocked meteorites of similar chondrite type and reasonable size were selected for the present purpose. Yamato-790964 is a seriously shocked LL chondrite whose schematic figure is shown in Fig. 1. From this chondrite, three portions, 97 (outer part; 0.7821 g), 67 (outer part; 0.8088 g) and 96 (inner part; 0.7542 g) were taken. Under a microscope, this meteorite shows a sign of impact-melt, indicating a serious shock effect for this meteorite (NAKAMURA and OKANO, 1985). In effect, a

---

\* Present address: Earthquake Research Institute, University of Tokyo, 1-1, Yayoi 1-chome, Bunkyo-ku, Tokyo 113.

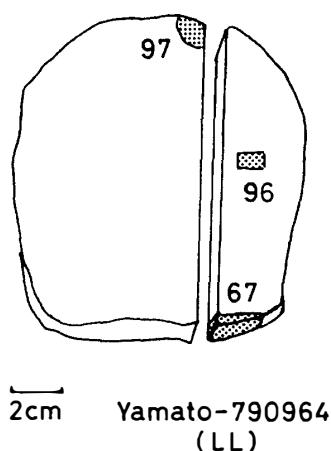


Fig. 1. The schematic sketch of the cut surface of the shocked meteorite Y-790964 (LL). The number indicates each portion used for the present study.

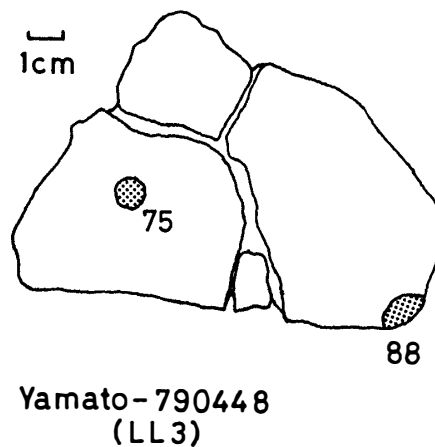


Fig. 2. The schematic sketch of the cut surface of the unshocked meteorite Y-790448 (LL3). The meaning of numerical figures is the same as in Fig. 1.

Rb-Sr isochron age of  $1197 \pm 54$  Ma was reported for this meteorite as the time of the shock event (NAKAMURA and OKANO, 1985).

An unshocked LL3 chondrite, Y-790448 was also examined for comparison. In Fig. 2, the schematic figure of this meteorite is shown. From this meteorite, two portions 88 (outer part; 0.7892 g) and 75 (inner part; 0.8056 g) were adopted for the present purpose.

No fusion crust was included in each sample.

### 3. Experimental Procedures

Each sample was wrapped in aluminium foil. They were stacked in quartz tubes together with age standards MMhb-1 (hornblende, K-Ar age:  $519.5 \pm 2.5$  Ma) (ALEXANDER *et al.*, 1978) for monitoring the neutron flux gradients. Remelted  $\text{CaF}_2$  and  $\text{K}_2\text{SO}_4$  were also included to monitor Ca- and K-derived interference correction factors.

Samples were irradiated in the JMTR of Tohoku University with the total fast neutron flux of about  $7 \times 10^{18}$  n/cm<sup>2</sup>. After Ar gas was extracted, Ar isotopes were analyzed on a Quadrupole Mass Spectrometer (TAKIGAMI *et al.*, 1984).

Before each sample analysis, blanks were taken and applied to the correction of the data. Blank levels are  $(3-10) \times 10^{-9}$  cm<sup>3</sup> STP <sup>40</sup>Ar except for Y-790964,97, whose blank level is  $(2-3) \times 10^{-8}$  cm<sup>3</sup> STP <sup>40</sup>Ar for 45 min heating time.

The amounts of Ar were estimated from the sensitivity of the mass spectrometer deduced from the amount of radiogenic <sup>40</sup>Ar in the standard sample. About 20% uncertainty is assigned on the basis of reproducibility.

The analyses of  $\text{CaF}_2$  and  $\text{K}_2\text{SO}_4$  gave the following values as the correction factors for Ca- and K-derived interference Ar isotopes.

$$(^{39}\text{Ar}/^{37}\text{Ar})_{\text{Ca}} = (1.25 \pm 0.06) \times 10^{-3},$$

$$(^{38}\text{Ar}/^{37}\text{Ar})_{\text{Ca}} = (2.89 \pm 0.15) \times 10^{-3},$$

$$(^{36}\text{Ar}/^{37}\text{Ar})_{\text{Ca}} = (4.36 \pm 0.22) \times 10^{-4},$$

$$({}^{40}\text{Ar}/{}^{39}\text{Ar})_{\text{K}} = (1.80 \pm 0.09) \times 10^{-1}$$

and

$$({}^{38}\text{Ar}/{}^{39}\text{Ar})_{\text{K}} = (3.00 \pm 0.15) \times 10^{-2}.$$

The amounts of trapped and spallogenic components were calculated by assuming that the  ${}^{38}\text{Ar}/{}^{39}\text{Ar}$  ratios for trapped and spallogenic components are 0.187 and 1.5, respectively.  ${}^{40}\text{Ar}$  was corrected for trapped ( ${}^{40}\text{Ar}/{}^{39}\text{Ar} = 0.5 \pm 0.5$ ) and spallogenic ( ${}^{40}\text{Ar}/{}^{39}\text{Ar} = 0.15 \pm 0.15$ ) components (PODOSEK and HUNEKE, 1973). When the  ${}^{38}\text{Ar}/{}^{39}\text{Ar}$  ratio exceeds 1.5, the excess  ${}^{38}\text{Ar}$  is assumed to have been produced by the reaction  ${}^{37}\text{Cl} (n, \gamma\beta) {}^{38}\text{Ar}$ , and the remainder spallogenic. However, this assumption seems to be not always guaranteed in the present case due to a relatively high neutron flux on samples. Hence, no exposure ages are reported in the present study.

Such experimental procedures for the greater part are the same as those reported before (KANEOKA, 1980, 1981, 1983).

#### 4. Results

The observed Ar isotopic ratios and the amount of  ${}^{40}\text{Ar}$  for each temperature fraction are shown in Table 1. Blanks in the extraction system and backgrounds in the mass spectrometer+gas introduction system were subtracted and the radioactive decay of  ${}^{37}\text{Ar}$  was also corrected. The data except for the  ${}^{40}\text{Ar}/{}^{39}\text{Ar}$  ratio represent those before correcting for Ca- and K-derived interference isotopes.  ${}^{40}\text{Ar}$ - ${}^{39}\text{Ar}$  ages are shown in the last column of Table 1. The assigned uncertainties in the observed Ar isotopic ratios are calculated based on the data of the maximum and the minimum contributions from the blank and background subtractions.

##### 4.1. Y-790964 (LL, shocked)

In Figs. 3a-3c,  ${}^{40}\text{Ar}$ - ${}^{39}\text{Ar}$  age diagrams are shown together with the  ${}^{40}\text{Ar}/{}^{39}\text{Ar}$ - ${}^{39}\text{Ar}/{}^{39}\text{Ar}$  isochron plots. As seen in these figures, the age spectra of the inner part (Y-790964,96) and two outer parts (Y-790964,97 and 67) indicate similar patterns, though that of Y-790964,97 is a little more scattered than that of Y-790964,96.

The observed ages decrease gradually in the higher temperature fractions except for the 1200°C fractions which might represent the redistribution of Ar to some extent at the time of shock event. The problem about the apparent young age observed in the 1200°C fraction is discussed in the next section.

In the lower and intermediate temperature fractions, plateau ages of  $1241 \pm 37$  Ma (600-1100°C fractions; 58.9% of the released  ${}^{39}\text{Ar}$ ),  $1264 \pm 23$  Ma (700-1000°C fractions; 41.2% of the released  ${}^{39}\text{Ar}$ ) and  $1276 \pm 24$  Ma (600-1100°C fractions; 64.7% of the released  ${}^{39}\text{Ar}$ ) are observed for samples Y-790964,97,67 and 96, respectively. Total fusion ages are  $1208 \pm 59$  Ma (Y-790964,97),  $1257 \pm 26$  Ma (Y-790964,67) and  $1240 \pm 29$  Ma (Y-790964,96). Since they show almost the same age within these analytical uncertainties and the age decrease in the higher temperature fractions is very small, they probably represent the age of the shocked event. Moreover, they agree with the reported Rb-Sr age ( $1197 \pm 54$  Ma) for the same chondrite within each uncertainty range (NAKAMURA and OKANO, 1985). The apparent  ${}^{40}\text{Ar}$ - ${}^{39}\text{Ar}$  age in the 600°C

Table 1. Ar isotopes in neutron-irradiated meteorite samples from Antarctica.

Y-790964,67 (LL) 0.8088 g  $J=0.05970\pm0.00130$ 

T (°C)	$\frac{^{40}\text{Ar}}{(\times 10^{-7} \text{ cm}^3 \text{ STP/g})}$	$\frac{^{36}\text{Ar}}{^{40}\text{Ar}} (\times 10^{-4})$	$\frac{^{37}\text{Ar}}{^{40}\text{Ar}} (\times 10^{-2})$	$\frac{^{38}\text{Ar}}{^{40}\text{Ar}} (\times 10^{-2})$	$\frac{^{39}\text{Ar}}{^{40}\text{Ar}} (\times 10^{-2})$	$^{40}\text{Ar}^*/^{39}\text{Ar}^*$	Age** (Ma)
600	3.67	12.73 $\pm 0.50$	2.397 $\pm 0.677$	1.743 $\pm 0.019$	4.333 $\pm 0.043$	22.87 $\pm 0.27$	1553 $\pm 26$
700	4.02	4.168 $\pm 0.334$	3.526 $\pm 0.643$	2.183 $\pm 0.022$	5.752 $\pm 0.052$	17.21 $\pm 0.19$	1275 $\pm 22$
800	3.09	5.152 $\pm 0.401$	6.353 $\pm 0.663$	2.582 $\pm 0.033$	5.884 $\pm 0.064$	16.84 $\pm 0.22$	1255 $\pm 23$
900	2.89	6.737 $\pm 0.497$	5.845 $\pm 0.774$	3.482 $\pm 0.050$	5.831 $\pm 0.076$	16.98 $\pm 0.24$	1263 $\pm 24$
1000	0.600	13.79 $\pm 2.36$	n.d.***	4.642 $\pm 0.263$	5.916 $\pm 0.332$	16.71 $\pm 0.97$	1249 $\pm 56$
1100	0.464	15.06 $\pm 3.69$	27.92 $\pm 11.80$	6.666 $\pm 0.568$	6.737 $\pm 0.575$	14.73 $\pm 1.35$	1139 $\pm 79$
1200	0.600	21.63 $\pm 3.58$	42.65 $\pm 6.11$	9.186 $\pm 0.733$	7.826 $\pm 0.622$	12.67 $\pm 1.05$	1016 $\pm 67$
1300	1.20	48.42 $\pm 3.19$	101.7 $\pm 6.0$	13.18 $\pm 0.62$	6.838 $\pm 0.320$	14.69 $\pm 0.78$	1136 $\pm 49$
1600	6.24	64.30 $\pm 1.33$	130.1 $\pm 2.3$	13.89 $\pm 0.18$	6.572 $\pm 0.083$	15.38 $\pm 0.29$	1175 $\pm 25$
Total	22.8	25.74 $\pm 0.97$	45.30 $\pm 1.63$	6.458 $\pm 0.115$	5.912 $\pm 0.103$	16.88 $\pm 0.31$	1257 $\pm 26$
Plateau age**		1264 $\pm$ 23 Ma (700–1000°C; 41.2% of released $^{39}\text{Ar}$ )					

Y-790964,96 (LL) 0.7542 g  $J=0.06096\pm0.00132$ 

T (°C)	$\frac{^{40}\text{Ar}}{(\times 10^{-7} \text{ cm}^3 \text{ STP/g})}$	$\frac{^{36}\text{Ar}}{^{40}\text{Ar}} (\times 10^{-4})$	$\frac{^{37}\text{Ar}}{^{40}\text{Ar}} (\times 10^{-2})$	$\frac{^{38}\text{Ar}}{^{40}\text{Ar}} (\times 10^{-2})$	$\frac{^{39}\text{Ar}}{^{40}\text{Ar}} (\times 10^{-2})$	$^{40}\text{Ar}^*/^{39}\text{Ar}^*$	Age** (Ma)
600	3.45	6.167 $\pm 0.633$	2.302 $\pm 1.225$	1.947 $\pm 0.036$	5.585 $\pm 0.099$	17.73 $\pm 0.35$	1322 $\pm 27$
700	1.49	3.584 $\pm 1.204$	2.178 $\pm 2.179$	2.204 $\pm 0.074$	5.936 $\pm 0.198$	16.68 $\pm 0.63$	1265 $\pm 40$
800	2.17	4.825 $\pm 0.773$	3.018 $\pm 1.646$	2.677 $\pm 0.054$	5.989 $\pm 0.118$	16.52 $\pm 0.38$	1257 $\pm 29$
900	3.02	7.527 $\pm 0.563$	9.451 $\pm 1.357$	3.743 $\pm 0.056$	5.904 $\pm 0.085$	16.79 $\pm 0.27$	1271 $\pm 25$
1000	1.47	13.16 $\pm 0.99$	13.31 $\pm 2.30$	7.175 $\pm 0.160$	5.962 $\pm 0.129$	16.63 $\pm 0.40$	1263 $\pm 29$
1100	0.960	20.49 $\pm 1.89$	18.38 $\pm 3.15$	13.48 $\pm 0.53$	6.297 $\pm 0.246$	15.74 $\pm 0.66$	1213 $\pm 42$
1200	0.798	25.35 $\pm 2.77$	33.72 $\pm 4.16$	14.61 $\pm 0.76$	7.403 $\pm 0.384$	13.39 $\pm 0.77$	1077 $\pm 50$
1300	1.34	48.90 $\pm 2.55$	106.9 $\pm 5.5$	13.50 $\pm 0.48$	6.692 $\pm 0.236$	15.04 $\pm 0.60$	1174 $\pm 39$
1600	3.97	76.27 $\pm 2.08$	176.7 $\pm 4.5$	14.57 $\pm 0.29$	6.627 $\pm 0.128$	15.38 $\pm 0.38$	1193 $\pm 29$
Total	18.7	26.13 $\pm 1.26$	51.22 $\pm 2.51$	7.409 $\pm 0.172$	6.157 $\pm 0.142$	16.21 $\pm 0.38$	1240 $\pm 29$
Plateau age**		1276 $\pm$ 24 Ma (600–1100°C; 64.7% of released $^{39}\text{Ar}$ )					

Table 1 (continued).

Y-790964,97 (LL) 0.7821 g  $J=0.06226\pm0.00135$ 

T (°C)	$\frac{^{40}\text{Ar}}{(\times 10^{-7} \text{ cm}^3 \text{ STP/g})}$	$\frac{^{38}\text{Ar}/^{40}\text{Ar}}{(\times 10^{-4})}$	$\frac{^{37}\text{Ar}/^{40}\text{Ar}}{(\times 10^{-2})}$	$\frac{^{38}\text{Ar}/^{40}\text{Ar}}{(\times 10^{-2})}$	$\frac{^{39}\text{Ar}/^{40}\text{Ar}}{(\times 10^{-2})}$	$^{40}\text{Ar}^*/^{38}\text{Ar}^*$	Age** (Ma)
600	4.18	7.583 $\pm 1.777$	1.719 $\pm 0.571$	2.318 $\pm 0.117$	6.127 $\pm 0.307$	16.14 $\pm 0.87$	1255 $\pm 53$
700	2.19	2.534 $\pm 2.542$	2.371 $\pm 1.164$	2.237 $\pm 0.185$	6.413 $\pm 0.529$	15.42 $\pm 1.32$	1214 $\pm 78$
800	1.52	2.818 $\pm 2.830$	3.365 $\pm 1.493$	2.532 $\pm 0.249$	6.639 $\pm 0.649$	14.90 $\pm 1.51$	1184 $\pm 90$
900	1.98	5.226 $\pm 2.132$	n.d.***	29.19 $\pm 0.189$	6.296 $\pm 0.401$	15.70 $\pm 1.03$	1230 $\pm 62$
1000	2.14	9.267 $\pm 1.647$	9.862 $\pm 1.274$	4.147 $\pm 0.179$	5.787 $\pm 0.248$	17.13 $\pm 0.80$	1310 $\pm 48$
1100	1.08	13.78 $\pm 3.64$	13.50 $\pm 2.40$	8.529 $\pm 0.805$	6.286 $\pm 0.593$	15.77 $\pm 1.54$	1234 $\pm 89$
1200	0.568	23.25 $\pm 8.59$	46.41 $\pm 10.72$	12.09 $\pm 2.42$	8.501 $\pm 1.702$	11.66 $\pm 2.39$	984 $\pm 156$
1300	1.33	42.18 $\pm 5.62$	94.06 $\pm 9.55$	13.44 $\pm 1.31$	7.784 $\pm 0.756$	12.84 $\pm 1.31$	1060 $\pm 84$
1600	6.38	58.87 $\pm 2.67$	12.15 $\pm 4.39$	11.92 $\pm 4.12$	6.660 $\pm 0.230$	15.15 $\pm 0.61$	1198 $\pm 40$
Total	21.4	24.88 $\pm 2.76$	45.86 $\pm 3.11$	6.697 $\pm 0.415$	6.508 $\pm 0.402$	16.28 $\pm 0.97$	1208 $\pm 59$
Plateau age**		1241 $\pm$ 37 Ma (600–1100°C; 58.9% of released $^{39}\text{Ar}$ )					

Y-790448,75 (LL3) 0.8056 g  $J=0.06195\pm0.00071$ 

T (°C)	$\frac{^{40}\text{Ar}}{(\times 10^{-7} \text{ cm}^3 \text{ STP/g})}$	$\frac{^{38}\text{Ar}/^{40}\text{Ar}}{(\times 10^{-3})}$	$\frac{^{37}\text{Ar}/^{40}\text{Ar}}{(\times 10^{-2})}$	$\frac{^{38}\text{Ar}/^{40}\text{Ar}}{(\times 10^{-3})}$	$\frac{^{39}\text{Ar}/^{40}\text{Ar}}{(\times 10^{-3})}$	$^{40}\text{Ar}^*/^{38}\text{Ar}^*$	Age* (Ma)
600	66.2	0.8028 $\pm 0.0109$	0.7535 $\pm 0.0922$	16.80 $\pm 0.11$	5.490 $\pm 0.023$	182.2 $\pm 0.8$	4525 $\pm 20$
700	40.5	0.5273 $\pm 0.0086$	0.7835 $\pm 0.1176$	7.269 $\pm 0.042$	5.673 $\pm 0.027$	176.4 $\pm 0.9$	4472 $\pm 21$
800	19.2	0.6543 $\pm 0.0122$	1.155 $\pm 0.203$	6.700 $\pm 0.043$	5.669 $\pm 0.030$	176.6 $\pm 1.0$	4474 $\pm 21$
900	12.3	1.858 $\pm 0.033$	2.240 $\pm 0.426$	9.014 $\pm 0.074$	5.901 $\pm 0.051$	170.0 $\pm 1.7$	4411 $\pm 25$
1000	5.05	12.34 $\pm 0.19$	3.974 $\pm 1.385$	22.22 $\pm 0.23$	7.493 $\pm 0.078$	133.4 $\pm 2.2$	4016 $\pm 33$
1100	1.99	143.8 $\pm 3.0$	17.89 $\pm 3.17$	86.70 $\pm 1.57$	16.74 $\pm 0.32$	56.77 $\pm 4.25$	2720 $\pm 106$
1200	1.04	648.6 $\pm 21.6$	67.04 $\pm 6.72$	243.0 $\pm 7.6$	37.48 $\pm 1.16$	18.68 $\pm 8.80$	1387 $\pm 456$
1300	1.55	422.0 $\pm 10.2$	100.6 $\pm 5.1$	125.8 $\pm 2.8$	35.69 $\pm 0.79$	22.96 $\pm 6.34$	1596 $\pm 293$
1600	—	—	—	—	—	—	—
Total	148	12.07 $\pm 0.16$	2.788 $\pm 0.318$	16.08 $\pm 0.11$	6.358 $\pm 0.036$	157.1 $\pm 1.5$	4281 $\pm 24$
Plateau age**		4492 $\pm$ 20 Ma (600–900°C; 74.5% of released $^{39}\text{Ar}$ )					

Table 1 (continued).

Y-790448,88 (LL3) 0.7892 g  $J=0.06217 \pm 0.00071$ 

T (°C)	$\frac{(^{40}\text{Ar})}{(\times 10^{-7} \text{ cm}^3 \text{ STP/g})}$	$\frac{^{38}\text{Ar}/^{40}\text{Ar}}{(\times 10^{-3})}$	$\frac{^{37}\text{Ar}/^{40}\text{Ar}}{(\times 10^{-2})}$	$\frac{^{38}\text{Ar}/^{40}\text{Ar}}{(\times 10^{-3})}$	$\frac{^{39}\text{Ar}/^{40}\text{Ar}}{(\times 10^{-3})}$	$^{40}\text{Ar}^*/^{39}\text{Ar}^*$	Age** (Ma)
600	61.3	1.097 $\pm 0.013$	n.d.***	65.02 $\pm 0.36$	6.111 $\pm 0.029$	163.4 $\pm 0.8$	4351 $\pm 21$
700	37.7	0.6799 $\pm 0.0102$	0.8860 $\pm 0.1035$	12.77 $\pm 0.08$	5.899 $\pm 0.033$	169.6 $\pm 1.0$	4413 $\pm 21$
800	24.7	0.9595 $\pm 0.014$	n.d.***	11.11 $\pm 0.08$	6.843 $\pm 0.305$	145.8 $\pm 6.5$	4165 $\pm 75$
900	12.8	2.393 $\pm 0.034$	2.015 $\pm 0.225$	14.92 $\pm 0.12$	6.429 $\pm 0.044$	155.8 $\pm 1.3$	4274 $\pm 23$
1000	5.91	13.83 $\pm 0.17$	4.729 $\pm 0.75$	37.90 $\pm 0.28$	9.202 $\pm 0.057$	108.4 $\pm 1.4$	3692 $\pm 27$
1100	2.60	151.6 $\pm 2.3$	18.23 $\pm 1.63$	102.5 $\pm 12.2$	22.90 $\pm 0.27$	41.27 $\pm 2.66$	2294 $\pm 85$
1200	1.44	495.6 $\pm 11.4$	n.d.***	181.5 $\pm 38.4$	38.88 $\pm 0.82$	19.66 $\pm 6.06$	1440 $\pm 306$
1300	1.39	472.7 $\pm 12.5$	116.2 $\pm 4.7$	138.0 $\pm 34.6$	43.35 $\pm 1.09$	18.24 $\pm 5.91$	1367 $\pm 310$
1600	5.23	95.90 $\pm 1.79$	78.76 $\pm 2.04$	33.92 $\pm 0.54$	18.22 $\pm 0.28$	55.22 $\pm 3.42$	2686 $\pm 88$
Total	153	16.22 $\pm 0.26$	4.623 $\pm 0.193$	39.55 $\pm 0.26$	7.668 $\pm 0.085$	130.3 $\pm 1.7$	3983 $\pm 27$
Mean age**		4325 $\pm$ 24 Ma (600–900°C; 72.8% of released $^{39}\text{Ar}$ )					

The uncertainty represents one standard deviation. The uncertainties in ages and  $^{40}\text{Ar}^*/^{39}\text{Ar}^*$  ratios do not include those of correction factors for Ca- and K-derived interference Ar isotopes.

\*  $^{40}\text{Ar}^*/^{39}\text{Ar}^*$  indicates a ratio of the radiogenic  $^{40}\text{Ar}$  from the decay of  $^{40}\text{K}$  ( $=^{40}\text{Ar}^*$ ) to the K-derived  $^{39}\text{Ar}$  by a reaction of  $^{39}\text{K}(n, p)^{39}\text{Ar}(=^{39}\text{Ar}^*)$ .

\*\*  $^{40}\text{Ar}-^{39}\text{Ar}$  ages were calculated by using following constants for  $^{40}\text{K}$  (STEIGER and JÄGER, 1977).  
 $\lambda_0 = 0.581 \times 10^{-10} \text{ yr}^{-1}$ ,  $\lambda_\beta = 4.962 \times 10^{-10} \text{ yr}^{-1}$ ,  $^{40}\text{K}/\text{K} = 1.167 \times 10^{-4}$ .

\*\*\* n.d. indicates “not determined” owing to the small amount of  $^{37}\text{Ar}$ .

fraction of Y-790964,67 is higher than those of Y-790964,96 and 97. This might be caused by terrestrial air contamination to the surface of the meteorite, because this portion is an outer part and no interference of  $^{40}\text{Ar}$  derived from the atmosphere was assumed in calculating each age.

In the isochron plots, reference isochrons corresponding to plateau ages are drawn in the  $^{40}\text{Ar}/^{39}\text{Ar}-^{39}\text{Ar}/^{36}\text{Ar}$  plots, where the isochrons go through the zero. Since most data lie on the reference isochrons, it implies that the air contamination from the sample and the experiment procedure was very low except for the 600°C fraction of Y-790964,67.

#### 4.2. Sample Y-790448 (LL3, unshocked)

In Figs. 4a and 4b,  $^{40}\text{Ar}-^{39}\text{Ar}$  diagrams and isochron plots are shown. The 1600°C fraction of Y-790448,75 was lost due to the experimental failure. The age diagram is drawn by assuming the same rate of the released  $^{39}\text{Ar}$  at 1600°C as Y-790448,88.

The  $^{40}\text{Ar}-^{39}\text{Ar}$  age pattern of Y-790448,88 (outer) resembles that of Y-790448,75

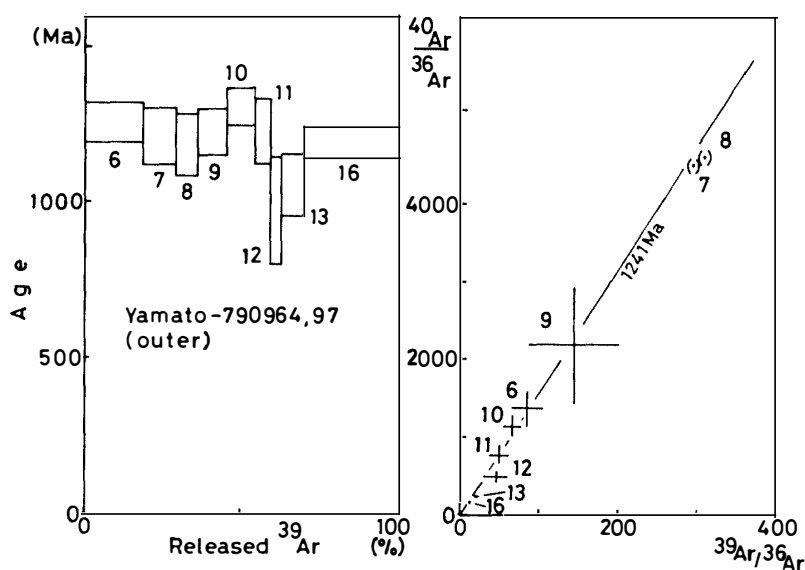


Fig. 3a. The  $^{40}\text{Ar}$ - $^{39}\text{Ar}$  age diagram and the  $^{40}\text{Ar}/^{36}\text{Ar}$ - $^{39}\text{Ar}/^{36}\text{Ar}$  plot for the shocked meteorite Y-790964,97 (LL; outer portion). The numerical figure at each column indicates the degassing temperature in hundred centigrade degrees. The uncertainties correspond to one standard deviation. In the right figure, the line of 1241 Ma, which indicates the plateau age in the left figure, is drawn as a reference which goes through the zero point.

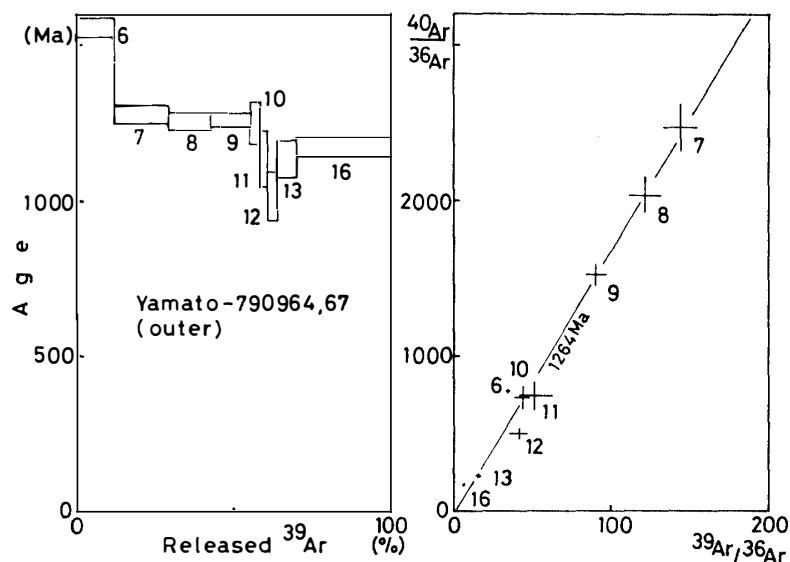


Fig. 3b. The  $^{40}\text{Ar}$ - $^{39}\text{Ar}$  age diagram and the  $^{40}\text{Ar}/^{36}\text{Ar}$ - $^{39}\text{Ar}/^{36}\text{Ar}$  plot for the shocked meteorite Y-790964,67 (LL; outer portion). The line of 1264 Ma is drawn as a reference.

(inner), but different from those of Y-790964. For the 600–900°C temperature fractions of Y-790448,75, we have a plateau age of  $4492 \pm 20$  Ma which constitutes 74.5% of released  $^{39}\text{Ar}$ . For Y-790448,88, the  $^{40}\text{Ar}$ - $^{39}\text{Ar}$  age pattern is slightly different from that of Y-790448,75, showing a slightly younger age in the 800°C fraction. The mean age for the 600–900°C temperature fractions is  $4325 \pm 24$  Ma (released  $^{39}\text{Ar}$ ; 72.8%). Total fusion ages are  $4281 \pm 24$  Ma and  $3983 \pm 27$  Ma for samples Y-790448,75 and

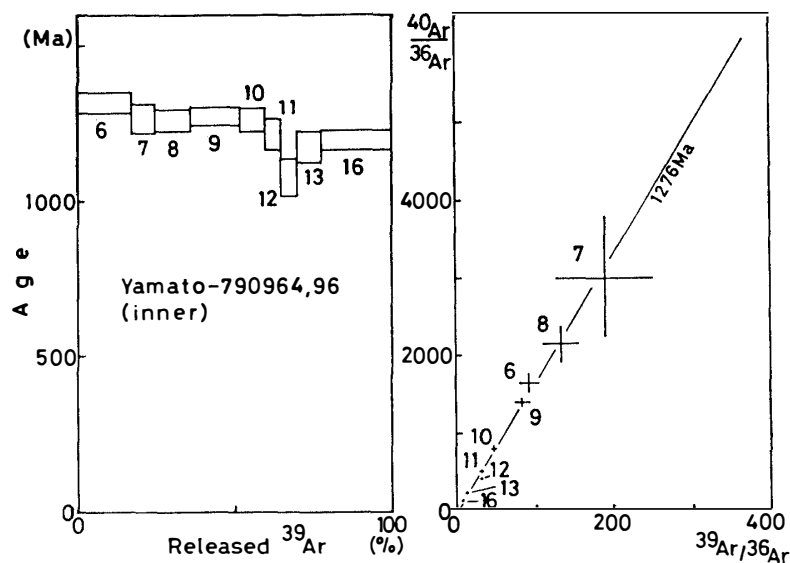


Fig. 3c. The  $^{40}\text{Ar}$ - $^{39}\text{Ar}$  age diagram and the  $^{40}\text{Ar}/^{36}\text{Ar}$ - $^{39}\text{Ar}/^{36}\text{Ar}$  plot for the shocked meteorite Y-790964,96 (LL; inner portion). The line of 1276 Ma is drawn as a reference.

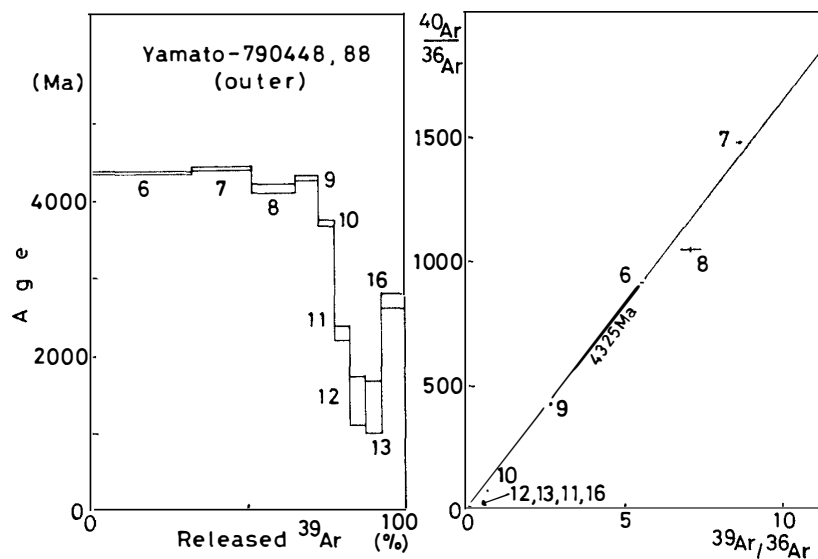


Fig. 4a. The  $^{40}\text{Ar}$ - $^{39}\text{Ar}$  age diagram and the  $^{40}\text{Ar}/^{36}\text{Ar}$ - $^{39}\text{Ar}/^{36}\text{Ar}$  plot for the unshocked meteorite Y-790448,88 (LL3; outer portion). The line of 4325 Ma, which indicates the mean age in the 600–900°C temperature fractions in the left figure, is drawn as a reference.

Y-790448,88, respectively. Although this meteorite is reported to be an unshocked meteorite, the total fusion age of Y-790448,75 is slightly older than Y-790448,88. This might be caused by some secondary effects such as weathering and so on.

The large decrease in age is observed for the temperature fractions above 1000°C in the age spectrum. This problem is discussed in the next section.

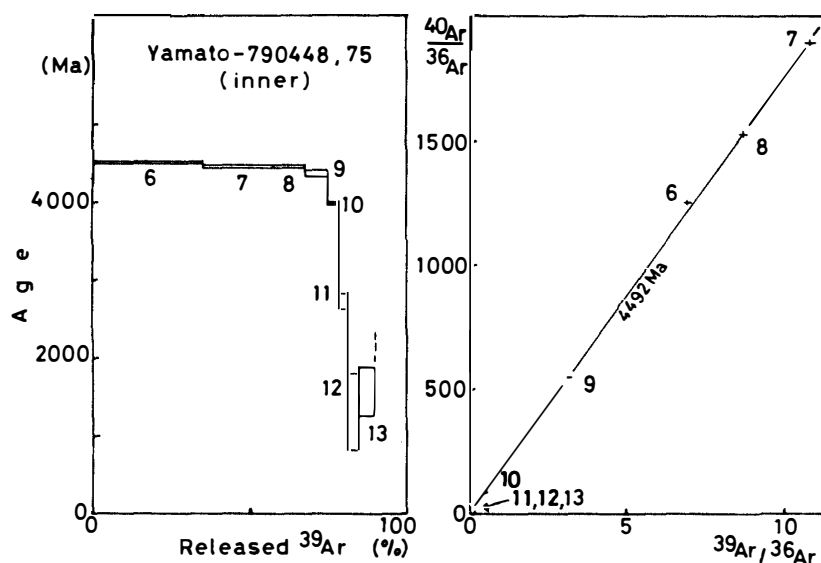


Fig. 4b. The  $^{40}\text{Ar}$ - $^{39}\text{Ar}$  age diagram and the  $^{40}\text{Ar}/^{36}\text{Ar}$ - $^{39}\text{Ar}/^{36}\text{Ar}$  plot for the unshocked meteorite Y-790448,75 (LL3; inner portion). The line of 4492 Ma, which indicates the plateau age in the left figure, is drawn as a reference.

## 5. Discussion

As shown in the previous section, the shocked meteorite Y-790964 shows almost the same plateau and total  $^{40}\text{Ar}$ - $^{39}\text{Ar}$  ages in the inner part and the outer part. This means that the shock affected the meteorite almost to the same degree in this size. Hence even if we used a portion of a meteorite sample of this size for the K-Ar and  $^{40}\text{Ar}$ - $^{39}\text{Ar}$  dating, the obtained age might be regarded as a representative one for the meteorite.

Further, it is worth-while to mention that the complete resetting of Ar occurred in this meteorite as revealed by the  $^{40}\text{Ar}$ - $^{39}\text{Ar}$  age patterns. In the  $^{40}\text{Ar}$ - $^{39}\text{Ar}$  age diagrams, even the highest temperature fractions show the relatively young ages which are similar to those observed in the lower temperature fractions. For a shocked LL-chondrite, old ages are often observed in the higher temperature fractions even if the age of lower temperature fractions represents that of the shock event (KANEOKA, 1981; BOGARD *et al.*, 1976). Hence, this complete resetting of Ar in Y-790964 would indicate a very intense shock event. This is compatible with the inferred reset of the Rb-Sr systematics.

BOGARD and HIRSCH (1980) reported that the release of  $^{39}\text{Ar}$  in the higher temperature fractions of very strongly reheated chondrites is larger than that of unshocked or moderately reheated chondrites. The released fraction of  $^{39}\text{Ar}$  of the shocked meteorite Y-790964 is clearly larger than that of the unshocked meteorite Y-790448 and this feature also suggests that a very strong shock event had affected Y-790964.

For Y-790964, all portions show slightly younger ages in the 1200°C fraction compared with other fractions. To explain this phenomenon, the occurrence of some secondary minerals might be considered, which were recrystallized slowly from shock-produced glass and degassed in the relatively high temperature fraction during a de-

gassing experiment. The apparent age gap between the time of shock event and the observed age in the 1200°C fraction might be explained as the time to form secondary mineral until it can keep radiogenic  $^{40}\text{Ar}$  after the shock event. Such feature has been recognized in a severely shocked lunar basalt (KIRSTEN and HORN, 1974).

In the sample Y-790448 (LL3, unshocked), characteristic  $^{40}\text{Ar}$ - $^{39}\text{Ar}$  age patterns are observed. In the lower temperature fractions, old ages, which might be close to the original age of this meteorite, are observed, whereas higher temperature fractions show much younger ages. Such a pattern is often observed in the LL-chondrite (TURNER *et al.*, 1978). In this case, however, this pattern is interpreted to show the recoil effect during the neutron irradiation for some samples because that they show a total fusion age of about 4500 Ma. Hence, further assumptions would be required to explain this age pattern of Y-790448.

Ages observed in the lower temperature fractions might correspond to the original  $^{40}\text{Ar}$ - $^{39}\text{Ar}$  ages, but the present results show slightly different  $^{40}\text{Ar}$ - $^{39}\text{Ar}$  ages between the inner and outer parts. Although the difference is not large, the apparent age difference exceeds the uncertainty of each value. The difference of the sampling portion might influence this result to some extent.

Further work is required to settle these problems for Y-790448.

### Acknowledgments

We appreciate the kindness of Prof. T. NAGATA and Dr. K. YANAI of the National Institute of Polar Research in providing us the samples used in this study. We are also grateful to the staff of Radioisotope Center, the University of Tokyo, who facilitated the Ar gas extraction. This study is financially supported in part by the Grant-in-Aid for Cooperative Research (No. 59390007) from the Ministry of Education, Science and Culture, Japan.

### References

- ALEXANDER, E. C., Jr., MICKELSON, G. M. and LANPHERE, M. A. (1978): MMhb-1; A new  $^{40}\text{Ar}$ - $^{39}\text{Ar}$  dating standard. U.S. Geol. Surv. Open-File Rep., **78-701**, 6-9.
- BOGARD, D. D. and HIRSCH, W. C. (1980):  $^{40}\text{Ar}/^{39}\text{Ar}$  dating, Ar diffusion properties, and cooling rate determinations of severely shocked chondrites. *Geochim. Cosmochim. Acta*, **44**, 1667-1682.
- BOGARD, D. D., HUSAIN, L. and WRIGHT, R. J. (1976):  $^{40}\text{Ar}$ - $^{39}\text{Ar}$  dating of collisional events in chondrite parent bodies. *J. Geophys. Res.*, **81**, 5664-5678.
- KANEOKA, I. (1980):  $^{40}\text{Ar}$ - $^{39}\text{Ar}$  ages of L and LL chondrites from Allan Hills, Antarctica; ALHA 77015, 77214 and 77304. *Mem. Natl Inst. Polar Res., Spec. Issue*, **17**, 177-188.
- KANEOKA, I. (1981):  $^{40}\text{Ar}$ - $^{39}\text{Ar}$  ages of Antarctic meteorites; Y-74191, Y-75258, Y-7308, Y-74450 and ALH-765. *Mem. Natl Inst. Polar Res., Spec. Issue*, **20**, 250-263.
- KANEOKA, I. (1983): Investigation of the weathering effect on the  $^{40}\text{Ar}$ - $^{39}\text{Ar}$  ages of Antarctic meteorites. *Mem. Natl Inst. Polar Res., Spec. Issue*, **30**, 259-274.
- KIRSTEN, T. and HORN, P. (1974): Chronology of the Taurus-Littrow region-III; Ages of mare basalts, and highland breccias and some remarks about the interpretation of lunar rock ages. *Proc. Lunar Sci. Conf.*, 5th, 1451-1475.
- NAKAMURA, N. and OKANO, O. (1985): 1200 Myr impact-melting age and trace-element chemical features of the Yamato-790964 chondrite. *Nature*, **315**, 563-566.

- PODOSEK, F. A. (1972): Gas retention chronology of Petersburg and other meteorites. *Geochim. Cosmochim. Acta*, **36**, 755–772.
- PODOSEK, F. A. and HUNEKE, J. C. (1973): Argon 40–argon 39 chronology of four calcium-rich achondrites. *Geochim. Cosmochim. Acta*, **37**, 667–684.
- STEIGER, R. H. and JÄGER, E. (1977): Subcommission on geochronology; Convention on the use of decay constants in geo- and cosmochronology. *Earth Planet. Sci. Lett.*, **36**, 359–362.
- TAKIGAMI, Y., NISHIJIMA, T., KOIKE, T. and OKUMA, K. (1984): Shijûkyoku shitsuryô bunsekikei no arugon 40–arugon 39 nendai sokuteihô e no ôyô (Application of quadrupole mass spectrometer to the  $^{40}\text{Ar}$ - $^{39}\text{Ar}$  geochronological study). *Shitsuryô Bunseki (Mass Spectroscopy)*, **89**, 227–233.
- TURNER, G., ENRIGHT, M. C. and CADOGAN, P. H. (1978): The early history of chondrite parent bodies inferred from  $^{40}\text{Ar}$ - $^{39}\text{Ar}$  ages. *Proc. Lunar Planet. Sci. Conf.*, 9th, 989–1025.

*(Received July 23, 1986; Revised manuscript received October 6, 1986)*